# Shear-Induced Orientation of Gyroid PS-b-P4VP(PDP) Supramolecules

Vukovic, Ivana; Friedrich, Heiner; Merino, Daniel Hermida; Portale, Giuseppe; ten Brinke, Gerrit; Loos, Katja

*Published in:*
Macromolecular Rapid Communications

*DOI:*
10.1002/marc.201300326



*Publication date:*
2013

# Shear-Induced Orientation of Gyroid PS-*b*-P4VP(PDP) Supramolecules

Ivana Vukovic, Heiner Friedrich, Daniel Hermida Merino, Giuseppe Portale, Gerrit ten Brinke,* Katja Loos*

The phase behavior of block copolymer based supramolecular complexes polystyrene-*block*-poly(4-vinylpyridine) (PS-*b*-P4VP) and amphiphilic pentadecylphenol (PDP) molecules resembles the phase behavior of conventional block copolymers. Several PS-*b*-P4VP(PDP) complexes are found to self-assemble into gyroid nanostructures. Typically, the grains are randomly oriented with a maximal size of several micrometers. Here, the orientation of a gyroid PS-*b*-P4VP(PDP) complex upon shearing is reported. It is found that the (111) gyroid lattice direction orients parallel to the shear direction after only several seconds of large amplitude oscillatory shearing. Oriented gyroid complexes can be used as templates for the preparation of metal nanofoams with improved ordering with potentially superior properties.

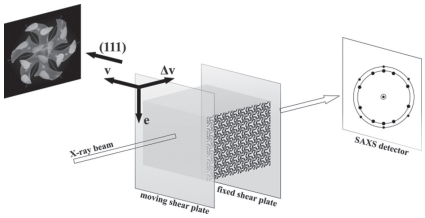


## 1. Introduction

Self-assembly of block copolymers has been extensively studied during the last decades.[1–3] Block copolymers with immiscible blocks can microphase separate and organize into various nanostructures (spherical, cylindrical, gyroid, lamellar, etc.) as a function of the composition, the architecture, the overall degree of polymerization, and the interaction. The periodicity of the block copolymer morphologies usually ranges from 10 to 100 nm and can be controlled by the overall degree of polymerization. Due to this, block copolymers are suitable candidates for nanofabrication purposes. For example, Lee et al. demonstrated the fabrication of ultrahigh density arrays of conducting polymer nanorods using block copolymer templates.[4] A mixture of poly(methyl methacrylate) (PMMA) homopolymer and polystyrene-*block*-poly(methyl methacrylate) (PS-*b*-PMMA) block copolymer was spin-coated onto a random copolymer coated ITO glass producing a thin film with the cylindrical morphology. Subsequently, PMMA homopolymer was removed by rinsing with acetic acid and the resulting nanoholes were backfilled with conducting polymer. Finally, the PS-*b*-PMMA matrix was dissolved in toluene, leaving behind arrays of conducting polymer oriented normal to the substrate surface, which have potential applications as sensor materials, nanoactuators, and organic photovoltaic devices. Gyroid-forming block copolymers in particular have attracted great attention for nanotechnological applications.[5–10] For instance, Crossland et al. utilized gyroid poly(4-fluorostyrene)-*block*-poly(d,l-lactide) (PFS-*b*-PLA) diblock copolymer to obtain bicontinuous bulk hetereojunction solar cell.[6] Vignolini et al. prepared an optical metamaterial—single gyroid, nanoscale ordered gold starting from triblock copolymer polyisoprene-*block*-polystyrene-*block*-polyethylene oxide (PI-*b*-PS-*b*-PEO).[10] Recently, our group demonstrated the application of gyroid-forming supramolecular block

Dr. I. Vukovic, Prof. G. ten Brinke, Prof. K. Loos
Department of Polymer Chemistry, Zernike Institute for Advanced Materials, University of Groningen, Nijenborgh 4, 9747, AG, Groningen, The Netherlands
E-mail: g.ten.brinke@rug.nl; k.u.loos@rug.nl
Dr. H. Friedrich
Department of Chemical Engineering and Chemistry, Laboratory of Materials and Interface Chemistry and CryoTEM Research Unit, Eindhoven University of Technology, P.O. Box 513, 5600 MB, Eindhoven, The Netherlands
Dr. D. Hermida-Merino, Dr. G. Portale
Netherlands Organization for Scientific Research, DUBBLE beamline at the ESRF, 6 rue Jules Horowitz, BP 220, 38043, CEDEX 9, Grenoble, France
Dr. D. Hermida-Merino
Dutch Polymer Institute, P.O. Box 902, 5600 AX, Eindhoven, The Netherlands.




DOI: 10.1002/marc.201300326

copolymer-based complexes polystyrene-*block*-poly(4-vinylpyridine)(pentadecylphenol) (PS-*b*-P4VP(PDP)) as precursors to well-ordered metallic nanofoams.[8] PS-*b*-P4VP(PDP) supramolecular complexes have been extensively studied in the group of Ikkala and our group.[11–16] Each PDP molecule contains a hydroxyl group and can form a hydrogen bond with a pyridine group of a P4VP repeating unit. Carefully selecting the composition of a starting block copolymer and the amount of added PDP, we prepared supramolecular complexes with double gyroid morphology. Subsequently, PDP was selectively dissolved in ethanol and metal was deposited in the remaining nanochannels. After the PS-*b*-P4VP removal by pyrolysis, metal nanofoams with inverse gyroid morphology were obtained that can possibly be applied in actuators, high power density batteries, hydrogen storage materials, etc. In contrast, alternative methods, such as dealloying, nanosmelting, sol–gel approach or combustion synthesis, render metal nanofoams with disordered structure.[17] Macroscopic functional properties of metal nanofoams emerge as a result of the interaction between the nanoligaments, which explains the importance of their nanostructural architecture. Although metal nanofoams prepared via block copolymer-templating approach show rather high degree of ordering, the maximal grain size is several cubic micrometers and grains have no preferential orientation. Oriented block copolymer templates will lead to metal nanofoams with improved ordering that might have superior properties, as actuators, for example, in comparison with the existing metal nanofoams.

It is well established that the long-range order of block copolymer structures can be induced by large amplitude oscillatory shear (LAOS).[18] In the lamellar phase, alternating layers may orient parallel, perpendicular, or transverse with respect to the shear plane. For instance, Stangler and Abetz[19] studied the orientation of lamellar polystyrene-*block*-polyisoprene (PS-*b*-PI) block copolymer upon LAOS. A perpendicular orientation was observed at 105 °C and low shearing frequencies. At higher frequencies a parallel orientation of the lamellae was found that developed either from a previously perpendicular or a previously transverse orientation. The transverse orientation was obtained in lamellar PS-*b*-PI block copolymers of intermediate molecular weight.[20] Moreover, hexagonal cylindrical phases can also be oriented by LAOS, exposing the (10) cylindrical planes parallel with respect to the shear plane (see Ref.[18] and references therein).

In a blend of polystyrene-*block*-poly(2-vinylpyridine) block copolymers, a oriented gyroid phase was found to develop from the shear-oriented hexagonal cylindrical phase.[21] The epitaxial relationship between the two phases was revealed. By shearing, (10) hexagonal planes of the cylindrical structure oriented parallel to the shear plane. On heating, the oriented gyroid phase was formed with a (111) direction along the shear direction. An epitaxial relationship between the hexagonally perforated layer (HPL) and the gyroid phase was also observed.[22] Vigild et al. studied the phase behavior of poly(ethylene-*alt*-propylene)-*block*-poly(dimethylsiloxane). Using isothermal time-resolved small-angle neutron scattering, they followed the transformation of the shear-oriented metastable HPL phase to the GYR phase. Additionally, they studied the isothermal growth of the GYR phase after quenching from a high-temperature shear-oriented CYL phase and the HPL appeared as a transitional phase.

Shear alignment of semi-crystalline block copolymers was studied by Fairclough et al.[23] Poly(ethylene oxide)-*block*-poly(butylene oxide) (PEO-*b*-PBO) block copolymer that adopted the GYR morphology in the melt state was oriented by oscillatory shear as confirmed by small-angle X-ray scattering (SAXS). Upon crystallization of the PEO block, a semicrystalline lamellar phase was formed. The lamellar planes retained the preferred directions of the oriented gyroid melt, but the domain spacing increased. Therefore, this transition was not defined as epitaxial, but it was rather concluded that the soft melt phase acted as a template for the hard crystalline phase.

## 2. Experimental Section

### 2.1. Materials

Diblock copolymer polystyrene-*block*-poly(4-vinylpyridine) ($\overline{M}_n$(PS) = 24 000 g mol$^{-1}$, $\overline{M}_n$(P4VP) = 9500 g mol$^{-1}$, PDI = 1.10) was obtained from Polymer Source Inc (Canade) and used as received. 3-Pentadecylphenol (PDP, 98%; Aldrich, Netherdlands) was recrystallized twice from petroleum ether. Chloroform (p.a., LAB-SCAN) was used as received.

### 2.2. Preparation of the Polymer Film

Film of the supramolecular complex was cast by dissolving the appropriate amounts of PS-*b*-P4VP diblock copolymer and PDP in chloroform. The concentration of polymer was maintained below 2 wt% to ensure homogeneous complex formation, and the solution was stirred for a couple of hours at room temperature. Afterward, the solution was poured into a glass Petri dish, which was subsequently placed into a saturated chloroform atmosphere. Chloroform was allowed to evaporate slowly during several days at room temperature. Subsequently, the sample was dried in vacuum at 30 °C overnight and heated for 30 min in an oven at 130 °C.

### 2.3. Characterization

Electron tomography (ET) was performed in annular dark-field (ADF) scanning transmission electron microscopy (STEM) mode using the TU/e CryoTitan. The CryoTitan, comprising a field emission gun and a Fischione high-angle ADF detector, was operated at 300 kV acceleration voltage. STEM images of the tomographic

tilt-series were recorded over an angular range of ±64 degrees at 1 degree increments with Xplore3D software (FEI Company, USA). To prepare the sample for ET, a piece of the film was embedded in epoxy resin (Epofix, Electron Microscopy Sciences) and cured overnight at 40 °C. The sample was subsequently microtomed to a thickness of 200 and 500 nm using a Leica Ultracut UCT-ultramicrotome and a Diatome diamond knife at room temperature. The microtomed sections were floated on water and subsequently placed on a copper grid. To obtain the contrast for ET, the sections were stained with iodine (45 min) that forms a complex with a pyridine ring. Thus, P4VP(PDP) block becomes stained and it appears bright in dark-field images. The microtomed sections are then labeled with 10 and 20 nm gold particles, which aid in the alignment of the tilt-series. Subsequently, the images of the tilt-series were aligned, binned to a final pixel size of 0.7 nm, and reconstructed (SIRT, 10 iterations) in IMOD.[24] Before 3D visualization using isosurface rendering in Avizo (VSG), results were denoised by nonlinear anisotropic diffusion.[24,25]

The PS-*b*-P4VP(PDP) supramolecular complex was examined by SAXS under in situ oscillatory shear. The sample was heated to 120 °C and sheared at 0.5 rad $s^{-1}$ frequency and 100% strain amplitude. SAXS was performed at the Dutch-Belgian Beamline (DUBBLE) station BM26B of the European Synchrotron Radiation Facility (ESRF) in Grenoble (France). The sample to detector distance was ca. 6 m with a wavelength of 1.033 Å. A Dectris-Pilatus 1M detector with a resolution of 981 × 1043 pixels and a pixel size of 172 × 172 μm was employed to record the 2D SAXS scattering patterns. Standard corrections for sample absorption and background subtraction were performed. The data were normalized with respect to the incident beam intensity in order to correct for primary beam intensity fluctuations. The scattering patterns from rat tail were used for the calibration of the wave vector scale of the scattering curve. The scattering vectorq was defined asq = $4\pi/\lambda \sin\theta$ with $2\theta$ being the scattering angle.[26,27] The 2D SAXS patterns were integrated using FIT2D software.

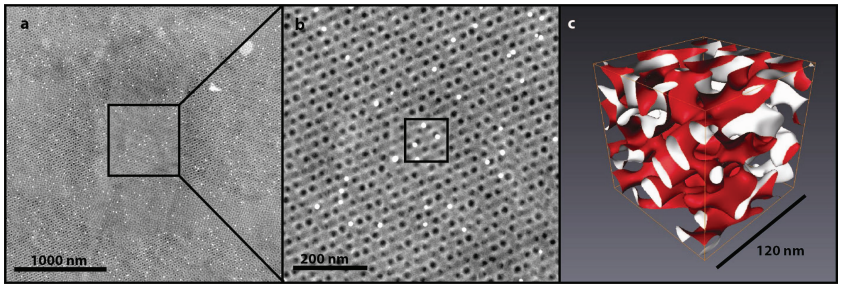


*Figure 1.* a,b) STEM images of double gyroid PS-*b*-P4VP(PDP) supramolecular complex and c) 3D analysis by ET.

## 3. Results and Discussion

Here, we examine the phase behavior of the gyroid PS-*b*-P4VP(PDP)$_x$ supramolecular complex under in situ oscillatory shear. In contrast to most of the previous studies, we directly shear a gyroid sample in order to improve its orientation. The supramolecular complex we use is prepared from PS-*b*-P4VP block copolymer with $\overline{M}_n$ (PS) = 24 000 g $mol^{-1}$, $\overline{M}_n$(P4VP) = 9500 g $mol^{-1}$, and $x$ = 1.0 ($x$ denote the ratio between PDP molecules and P4VP repeat units). The nanoscale ordering after phase separation has been examined in our previous study by TEM and SAXS.[15] The TEM micrograph presented in reference[15] displays the projection through the (110) gyroid plane. Its SAXS pattern contains the first two reflections in √6:√8 $q$ ratio and a nearly 10:1 intensity ratio, which represents the unambiguous signature of the double gyroid structure.[15,28] Here, we employ ET to elucidate the full 3D structure of the microphase separated domains before shearing (Figure 1). ET experiments were performed in dark-field STEM mode, hence the iodine stained P4VP(PDP)$_x$ domains appear bright in the images. Already from the electron micrographs shown in Figure 1a,b, the typical gyroid "wagon wheel" pattern, corresponding to a projection along the (111) gyroid direction can be discerned. The full 3D structure of the sample is depicted in Figure 1c. From the ET results it is clear that the sample has the ordered bicontinuous morphology. More information can be found in the Supporting Information, namely Video 1 detailing the co-continuous domains and Video 2 showing subsequent numerical cross-sections through the micrometer-sized gyroid grain.

To orient the gyroid morphology, the sample is heated above the glass transition temperature of the PS block and sheared *in situ* at a constant frequency (0.5 rad $s^{-1}$) and strain amplitude (100%). SAXS data are collected in

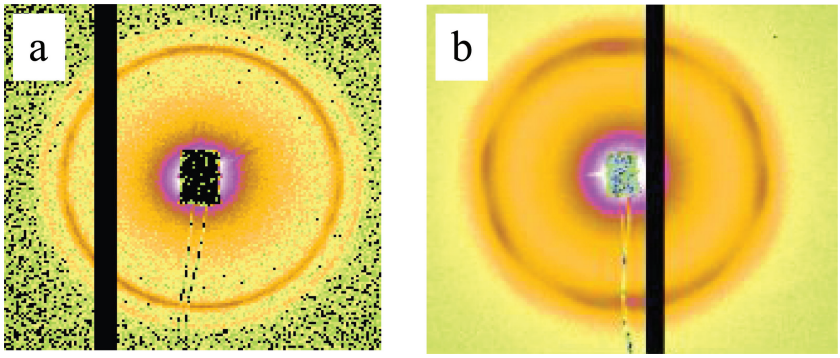


*Figure 2.* 2D diffraction patterns of PS-*b*-P4VP(PDP) complex with a double gyroid morphology. a) Before and b) after shearing at 120 °C, 0.5 rad $s^{-1}$ frequency, and 100% strain amplitude. The missing points (black stripe) correspond to the physical gaps of the detector.

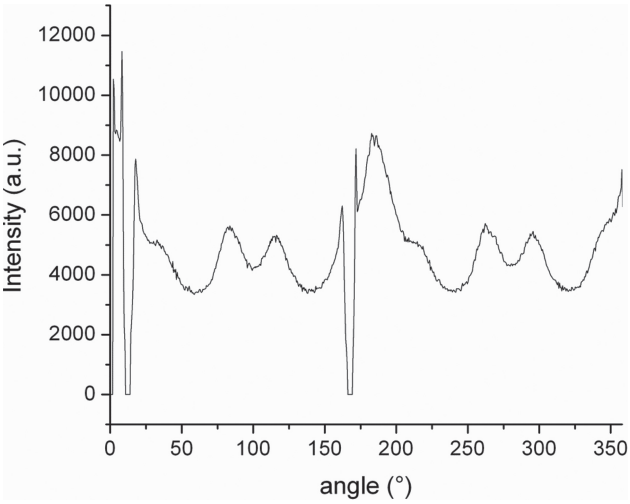


*Figure 3.* The azimuthal integration of the 2D diffraction pattern of the shear-oriented gyroid PS-*b*-P4VP(PDP) complex. The artificial spikes around 0° and 180° correspond to the physical gaps of the detector.

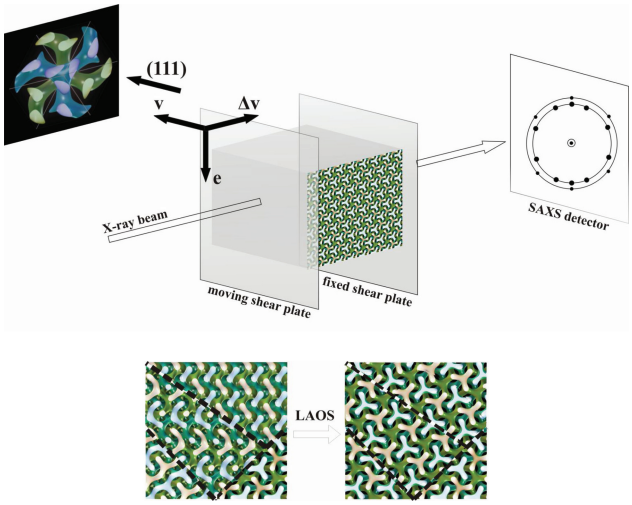


*Figure 4.* Schematic representation of shear-induced orientation of the gyroid PS-*b*-P4VP(PDP) complex. The gyroid phase aligns with the (111) direction parallel to the shear direction. Grains boundaries are not depicted in the schematic representation for the sake of simplicity. Its diffraction pattern consist of 10 first-order and six second-order spots originating from the families of (211) and (220) reflection planes, respectively. Shear direction (*v*), gradient direction (Δ*v*), and neutral direction (*e*) are displayed. TEM simulations are adapted from Ref [30]. Before LAOS, the gyroid sample consist of randomly oriented grains, and upon LAOS its orientation improves such that the (111) gyroid direction aligns parallel to the shear direction, as depicted in the two bottom images.

consecutive frames of 30 s duration. The 2D diffraction pattern of the unsheared gyroid sample (Figure 2a) contains two isotropic rings with the √6:√8 radii ratio that originate from (211) and (220) reflections planes, respectively. After a short time of LAOS (ca. 2–3 min), the diffraction pattern transforms to a 10-spot pattern reported for the shear-oriented gyroid samples.[22] The 2D SAXS of shear-oriented gyroid sample is collected over a time interval of 300 s and it is displayed in Figure 2b. The azimuthal integration of this pattern (Figure 3) reveals 6 distinct peaks and 4 shoulders originating from 10 first-order spots in the 2D diffraction pattern of the shear-oriented gyroid sample. The artificial spikes around 0° and 180° correspond to the physical gaps of the detector. Two peaks with the highest intensity appear at 4° and 184° and each has two shoulders at ±20°. The remaining four peaks have somewhat lower intensity and appear in pairs; the first pair is positioned at 83° and 116°, and the second one is 180° shifted (263° and 296°). This pattern suggests that the shear-oriented gyroid phase is aligned with the (111) lattice direction parallel to the shear direction as depicted in Figure 4. The characteristic diffraction pattern of the shear-oriented gyroid phase consists of ten first-order and six second-order spots originating from the families of (211) and (220) reflection planes, respectively. The first-order spots have higher intensity than the second-order ones, and therefore, are better resolved.[22,29] The oriented gyroid is not a single-crystal domain, but it consist of multiple domains rotated randomly around the (111) lattice directions. This characteristic 10-spot pattern arises from the rotation of single crystal domains by an angle θ around the (111) direction.

## 4. Conclusion

In this study, we examine the influence of LAOS on the orientation of the gyroid PS-*b*-P4VP(PDP) complexes. Despite the fact that oriented gyroid samples can be exploited for the preparation of materials with superior properties, the direct orientation of the gyroid phase has not been extensively studied yet. Before shearing the representative sample has an ordered bicontinuous gyroid morphology in relatively large areas/volumes as evidenced by ET. However, it is contains multiple grains, randomly oriented with a maximal size of several micrometers. The gyroid supramolecular PS-*b*-P4VP(PDP) complex responds promptly to the LAOS and orients with its (111) direction parallel to the shear direction as concluded from its 10-spot SAXS pattern characteristic for the oriented gyroid phase. In the future, the alignment kinetics and the influence of molecular parameters, such as block copolymer molar mass, or flow field parameters (strain amplitude, frequency) on the orientation will be examined in order to get a deeper understanding of this phenomenon.

In addition, the behavior of, for example, lamellar or cylindrical PS-*b*-P4VP(PDP) complexes upon LAOS can be compared with the behavior of the gyroid ones. Furthermore, the orientation of comb-block P4VP(PDP) and its

influence on the overall alignment can be studied. Such shear-oriented samples are promising candidates for the preparation of metal nanofoams with a high degree of ordering. These metallic nanostructures might have superior properties and perform better as actuators, for instance, in comparison with the existing ones. Therefore, this study opens a number of scientific questions that will be answered in the near future.

## Supporting Information

Supporting Information is available from the Wiley Online Library or from the author.

Acknowledgements: This project was financially supported by the Zernike Institute for Advanced Materials. Beamtime at DUBBLE (ESRF, Grenoble) has kindly been made available by The Netherlands Organization for Scientific Research (NWO). This work was financially supported through the Pieter Langerhuizen Stipendium awarded to Dr. Heiner Friedrich by the Koninklijke Hollandsche Maatschappij der Wetenschappen.

Received: April 8, 2013; Revised: June 8, 2013; Published online: July 9, 2013; DOI: 10.1002/marc.201300326

Keywords: block copolymers; gyroid morphology; oscillatory shearing; shear-induced ordering; supramolecular complexes

[1] F. S. Bates, G. H. Fredrickson, *Annu. Rev. Phys. Chem.* **1990**, *41*, 525.
[2] I. W. Hamley, *The Physics of Block Copolymers*, Oxford University Press, Oxford, **1998**.
[3] V. Abetz, P. Simon, *Phase Behaviour and Morphologies of Block Copolymers*, Springer Berlin / Heidelberg, **2005**, p. 125.
[4] J. I. Lee, S. H. Cho, S.-M. Park, J. K. Kim, J. K. Kim, J.-W. Yu, Y. C. Kim, T. P. Russell, *Nano Lett.* **2008**, *8*, 2315.
[5] A. M. Urbas, M. Maldovan, P. DeRege, E. L. Thomas, *Adv. Mater.* **2002**, *14*, 1850.
[6] E. J. W. Crossland, M. Kamperman, M. Nedelcu, C. Ducati, U. Wiesner, D. M. Smilgies, G. E. S. Toombes, M. A. Hillmyer, S. Ludwigs, U. Steiner, H. J. Snaith, *Nano Lett.* **2008**, *9*, 2807.
[7] H.-Y. Hsueh, H.-Y. Chen, M.-S. She, C.-K. Chen, R.-M. Ho, S. Gwo, H. Hasegawa, E. L. Thomas, *Nano Lett.* **2010**, *10*, 4994.
[8] I. Vukovic, S. Punzhin, Z. Vukovic, P. Onck, J. T. M. De Hosson, G. ten Brinke, K. Loos, *ACS Nano* **2011**, *5*, 6339.
[9] H.-Y. Hsueh, R.-M. Ho, *Langmuir* **2012**, *28*, 8518.
[10] S. Vignolini, N. A. Yufa, P. S. Cunha, S. Guldin, I. Rushkin, M. Stefik, K. Hur, U. Wiesner, J. J. Baumberg, U. Steiner, *Adv. Mater.* **2012**, *24*, OP23.
[11] J. Ruokolainen, G. ten Brinke, O. Ikkala, *Adv. Mater.* **1999**, *11*, 777.
[12] J. Ruokolainen, M. Saariaho, O. Ikkala, G. ten Brinke, E. L. Thomas, M. Torkkeli, R. Serimaa, *Macromolecules* **1999**, *32*, 1152.
[13] R. Mäki-Ontto, K. de Moel, W. de Odorico, J. Ruokolainen, M. Stamm, G. ten Brinke, O. Ikkala, *Adv. Mater.* **2001**, *13*, 117.
[14] O. Ikkala, G. ten Brinke, *Science* **2002**, *295*, 2407.
[15] I. Vukovic, T. P. Voortman, D. H. Merino, G. Portale, P. Hiekkataipale, J. Ruokolainen, G. ten Brinke, K. Loos, *Macromolecules* **2012**, *45*, 3503.
[16] I. Vukovic, G. ten Brinke, K. Loos, *Macromolecules* **2012**, *45*, 9409.
[17] B. C. Tappan, S. A. Steiner, E. P. Luther, *Angew. Chem. Int. Ed.* **2010**, *49*, 4544.
[18] I. W. Hamley, *J. Phys.: Condens. Matter* **2001**, *13*, R643.
[19] S. Stangler, V. Abetz, *Rheol. Acta* **2003**, *42*, 569.
[20] Y. Zhang, U. Wiesner, *J. Chem. Phys.* **1995**, *103*, 4784.
[21] M. F. Schulz, F. S. Bates, K. Almdal, K. Mortensen, *Phys. Rev. Lett.* **1994**, *73*, 86.
[22] M. E. Vigild, K. Almdal, K. Mortensen, I. W. Hamley, J. P. A. Fairclough, A. J. Ryan, *Macromolecules* **1998**, *31*, 5702.
[23] J. P. A. Fairclough, S.-M. Mai, M. W. Matsen, W. Bras, L. Messe, S. C. Turner, A. J. Gleeson, C. Booth, I. W. Hamley, A. J. Ryan, *J. Chem. Phys.* **2001**, *114*, 5425.
[24] J. R. Kremer, D. N. Mastronarde, J. R. McIntosh, *J. Struct. Biol.* **1996**, *116*, 71.
[25] A. S. Frangakis, R. Hegerl, *J. Struct. Biol.* **2001**, *135*, 239.
[26] M. Borsboom, W. Bras, I. Cerjak, D. Detollenaere, D. Glastra Van Loon, P. Goedtkindt, M. Konijnenburg, P. Lassing, Y. K. Levine, B. Munneke, M. Oversluizen, R. Van Tol, E. Vlieg, *J. Synchrotron. Radiat.* **1998**, *5*, 518.
[27] W. Bras, I. P. Dolbnya, D. Detollenaere, R. van Tol, M. Malfois, G. N. Greaves, A. J. Ryan, E. Heeley, *J. Appl. Crystallogr.* **2003**, *36*, 791.
[28] D. A. Hajduk, P. E. Harper, S. M. Gruner, C. C. Honeker, G. Kim, E. L. Thomas, L. J. Fetters, *Macromolecules* **1994**, *27*, 4063.
[29] S. Foerster, A. K. Khandpur, J. Zhao, F. S. Bates, I. W. Hamley, A. J. Ryan, W. Bras, *Macromolecules* **1994**, *27*, 6922.
[30] https://secure.msri.org/about/sgp/jim/software/temsim/index.html (accessed June, 2013).